



11-02
37 2000

TECHNICAL NOTE

D-339

EXPERIMENTAL AND THEORETICAL STUDY OF A RECTANGULAR
WING IN A VORTICAL WAKE AT LOW SPEED

By Willard G. Smith and Frank A. Lazzeroni

Ames Research Center
Moffett Field, Calif.

NATIONAL AERONAUTICS AND SPACE ADMINISTRATION
WASHINGTON

October 1960

NATIONAL AERONAUTICS AND SPACE ADMINISTRATION

TECHNICAL NOTE D-339

EXPERIMENTAL AND THEORETICAL STUDY OF A RECTANGULAR

WING IN A VORTICAL WAKE AT LOW SPEED

By Willard G. Smith and Frank A. Lazzeroni

SUMMARY

A systematic study has been made, experimentally and theoretically, of the effects of a vortical wake on the aerodynamic characteristics of a rectangular wing at subsonic speed. The vortex generator and wing were mounted on a reflection plane to avoid body-wing interference. Vortex position, relative to the wing, was varied both in the spanwise direction and normal to the wing. Angle of attack of the wing was varied from -4° to $+6^{\circ}$. Both chordwise and spanwise pressure distributions were obtained with the wing in uniform and vortical flow fields. Stream surveys were made to determine the flow characteristics in the vortical wake.

The vortex-induced lift was calculated by several theoretical methods including strip theory, reverse-flow theory, and reverse-flow theory including a finite vortex core. In addition, the Prandtl lifting-line theory and the Weissinger theory were used to calculate the spanwise distribution of vortex-induced loads. With reverse-flow theory, predictions of the interference lift were generally good, and with Weissinger's theory the agreement between the theoretical spanwise variation of induced load and the experimental variation was good. Results of the stream survey show that the vortex generated by a lifting surface of rectangular plan form tends to trail back streamwise from the tip and does not approach the theoretical location, or centroid of circulation, given by theory. This discrepancy introduced errors in the prediction of vortex interference, especially when the vortex core passed immediately outboard of the wing tip.

The wake produced by the vortex generator in these tests was not fully rolled up into a circular vortex, and so lacked symmetry in the vertical direction of the transverse plane. It was found that the direction of circulation affected the induced loads on the wing either when the wing was at angle of attack or when the vortex was some distance away from the plane of the wing.

INTRODUCTION

The problem of determining the aerodynamic characteristics of wings or tail surfaces in the flow field downstream of lifting surfaces has been the subject of much research. This problem has two basic parts: first, to determine the stream conditions in the wake of a lifting surface, and second, to evaluate the effect of this nonuniform stream on the trailing surface.

For canard configurations with the reduced wing span relative to tail span of many present-date configurations, the assumption of uniform downwash at the trailing surface is inadequate. Methods for estimating the development, rate of roll-up, and location of a vortical wake are given in references 1, 2, and 3. Most published experimental data concerning the effects of vortices on wings were obtained in the presence of bodies which introduce additional unknowns into the problem (see refs. 4 to 6).

The purpose of the present investigation was to study the effects of a vortex on a trailing wing under controlled conditions. Tests were made with a half-span rectangular wing in the wake of a vortex generator. Theoretical calculation of the wing loads was simplified by the use of a half-span model mounted on a reflection plane which eliminated the need for a body with its attendant crossflow. The wing was instrumented to measure local surface pressures in order to determine the chordwise and spanwise distribution of interference load. Extensive stream surveys were also made to determine the strength of the circulation and to locate the center of the vortical disturbance.

NOTATION

a_c radius of vortex core, ft

b wing span, ft

c local chord, ft

c_a average chord of wing, ft

c_l section lift coefficient

C_L lift coefficient, $\frac{L}{qS}$

(All lift coefficients are based on the area of the wing.)

C_{L_α} lift-curve slope, per deg

$\frac{C_{L_i}}{C_{L_G}}$	interference factor, ratio of interference lift on wing to lift produced by the vortex generator
L	lift force, lb
$\frac{\Delta p}{q}$	lifting pressure coefficient induced by vortex, $\frac{p_{\text{lower}} - p_{\text{upper}}}{q}$
q	free-stream dynamic pressure, lb/sq ft
s	y coordinate of wing tip, ft
S	wing area, sq ft
V	free-stream velocity, ft/sec
w	vertical component of wind velocity (positive downward), ft/sec
x,y,z	Cartesian coordinates, streamwise, spanwise, and vertical, respectively (fig. 1)
α	angle of attack, deg
ϵ	local downwash angle $\frac{w}{V}$, deg
Γ	circulation, sq ft/sec
ξ, η	variables of integration corresponding to x,y

Subscripts

i	induced effect
f	forward flow
r	reversed flow
v	vortex
G	vortex generator
W	wing

THEORETICAL METHODS

The influence of a vortical wake on a rectangular wing was calculated by several well-known methods for the purpose of assessing their relative merits by comparing theory with experimental results.

The limitations and assumptions used in the theoretical analyses are as follows:

1. Linearized theory was used assuming inviscid potential flow.
2. The load on a plain wing in nonuniform flow was assumed to be identical with the load on an appropriately twisted wing in uniform flow.
3. Infinite line vortex theory was used in order to express the nonuniform stream angle as a single mathematical expression. Neither the strength nor the path of the vortex was allowed to change in passing over the wing.

Wake Representation

To represent the wake, the forward lifting surface or vortex generator was replaced by a horseshoe vortex with the bound portion along the quarter-chord line with span $2y_v$ as defined by the Kutta-Joukowski theorem

$$L_G = \rho V \Gamma 2y_v \quad (1)$$

where the vortex span is obtained from the theoretical span load distribution (ref. 2).

A potential vortex with the tangential velocity inversely proportional to the distance from its center is, of course, unrealistic at the center. For some of the theoretical calculations, a rotational-core approximation as derived in reference 1 was used to eliminate this singularity in downwash distribution at the center. Further, the actual vortical wake may not be fully rolled up into a discrete vortex. The wake can then be more accurately represented by several horseshoe vortices, distributed according to the spanwise circulation distribution of the wing, as described in reference 2. However, in many practical cases a single horseshoe vortex adequately represents the wake.

Vortex-Induced Loads

The problem of determining the influence of a vortex on a wing is one of finding the lift on a wing in a nonuniform stream. One approach to this problem is the classical strip theory which considers each infinitesimal element of the wing to be independent from the others, and the induced lift coefficient is

$$C_{Li} = - \frac{c_{l\alpha}}{S} \int_{-S}^S \epsilon \, dy \quad (2)$$

where $c_{l\alpha}$ is the two-dimensional section lift coefficient per unit angle of attack. Strip theory gives quite erroneous answers, at least for untapered wings, when the vortex core passes near the wing tip since finite loads are predicted at the tip of the wing. However, when the vortex passes well inboard of the wing tip, strip theory may give reasonable answers since the errors are symmetrical and hence compensating about the vortex core.

Within the limitations and assumptions previously indicated, reverse-flow theory (ref. 7) can be applied to find the lift on a wing in a nonuniform flow field. If the downwash is considered to be constant in the chordwise direction and to vary in the spanwise direction, the induced lift coefficient given by this theory is:

$$C_{Li} = - \frac{C_{L\alpha} c_a}{S} \int_{-S}^S \epsilon_f \left(\frac{cc_l}{c_a C_{Lr}} \right) dy \quad (3)$$

where

$C_{L\alpha}$ three-dimensional lift-curve slope

$\frac{cc_l}{c_a C_{Lr}}$ span loading parameter in uniform flow

ϵ_f spanwise downwash distribution in forward flow

The reverse-flow theory is superior to the strip theory since it accounts for the variation in span load distribution due to wing plan form. However, neither theory defines the distribution of induced loads. The need for a solution to the problem of the distribution of induced loads suggests use of a lifting-surface theory.

Distribution of Induced Loads

An expression relating the lifting pressure on a wing to the local downwash angle has been derived by several investigators (refs. 8 and 9) using lifting-surface theory. In the notation of this paper, the equation is as follows. (It is assumed that the wing lies in the $z = 0$ plane.)

$$\left(\frac{w}{V}\right)_{x,y} = -\frac{1}{8\pi} \int_{-s}^s \int_0^c \frac{d}{d\eta} \left(\frac{\Delta p}{q}\right)_{\xi,\eta} \frac{d\xi d\eta}{y-\eta} \left[1 + \frac{\sqrt{(x-\xi)^2 + (y-\eta)^2}}{x-\xi}\right] \quad (4)$$

This equation has not been solved analytically to date; however, there are several simplifications which can be made that permit approximate solutions to the problem. One of these is Prandtl's lifting-line theory which is intended for large aspect-ratio wings; however, experience has shown that it is valid for aspect ratios as low as 3. The basic assumption in the lifting-line theory is that at each element of a finite wing the velocity distribution is identical to that for two-dimensional flow around the element with V' instead of V as the velocity at infinity, where

$$V' = \sqrt{V^2 + w^2}$$

The assumption of two-dimensional flow makes possible the evaluation of the chordwise loading and also, for large aspect-ratio wings, $(y-\eta)$ will generally be much larger than $(x-\xi)$ so $(y-\eta)$ may be substituted for $\sqrt{(x-\xi)^2 + (y-\eta)^2}$ in the lifting-surface equation. The spanwise variation of downwash may then be expressed as

$$w(y) = -\frac{1}{4\pi} \int_{-s}^s \frac{d\Gamma/d\eta}{y-\eta} d\eta \quad (5)$$

which is the Prandtl lifting-line integral equation expressed in terms of the circulation.

A method for obtaining a numerical solution of the lifting-line equation for a wing in nonuniform flow (presented in detail in ref. 10, p. 250) is summarized below. The spanwise variation of circulation is expressed as a trigonometric series of n terms, introducing the variables φ and θ by the substitutions

$$y = -s \cos \varphi, \quad \eta = -s \cos \theta$$

where s is the semispan of the wing. Then

$$\Gamma = 4sV (A_1 \sin \varphi + A_2 \sin 2\varphi + A_3 \sin 3\varphi + \dots + A_n \sin n\varphi) \quad (6)$$

The computations can be simplified by taking an odd number n of equidistant values of φ from 0 to π . Equations (5) and (6) can now be

combined to obtain a system of n linear equations with n unknowns. The local values of w/V must be specified at the n points. These may be experimental downwash angles or the values computed for potential line vortices. Solution of these equations gives the induced load at the n points.

The accuracy of the computed results depends on the number of control points used. In the present investigation an IBM 704 computing machine was used to compute the circulation distribution for 45 points along the semispan. Computing time was about 5 minutes and, the 45 control points were adequate to define the downwash distribution encountered in this investigation.

Another approximate solution to the lifting-surface equation is the Weissinger theory (L-method) which is similar to the Prandtl lifting-line theory. In the Weissinger theory (ref. 11) the lifting wing is replaced by a system of horseshoe vortices concentrated at the quarter chord, with a spanwise distribution such that the downwash at the $3/4$ -chord point will be equal and opposite to the corresponding component of the incident flow. Both mathematical models are consistent with the lifting-surface theory in the limit for infinite aspect ratio. As in Prandtl's theory, the two-dimensional chordwise lifting pressure variation was used. Since the boundary conditions are satisfied at

$x-\xi = c/2$, we may approximate the radical $\sqrt{(x-\xi)^2 + (y-\eta)^2}$ by $\sqrt{c^2/4 + (y-\eta)^2}$. With this simplification and after the terms are regrouped, equation (4) may be written

$$w(y) = - \frac{1}{4\pi} \left[\int_{-s}^s \frac{(d\Gamma/d\eta)d\eta}{y-\eta} + \frac{2}{c} \int_{-s}^s \frac{\sqrt{(c^2/4) + (y-\eta)^2}}{y-\eta} \frac{d\Gamma}{d\eta} d\eta \right] \quad (7)$$

An approximate solution for the spanwise distribution of circulation may be obtained in exactly the same manner as for the lifting-line theory (ref. 10). It is interesting to note that the equation for Weissinger's method (eq. (7)) is identical to Prandtl's equation (eq. (5)) except for the additional term on the right-hand side of the equation.

The solution of the simultaneous equations is somewhat more laborious because of the additional term. About 1-1/2 hours were required to compute the coefficients of the simultaneous equations on an electronic computer. However, for a given wing plan form these same coefficients may be used to compute any load conditions in only a few minutes.

APPARATUS

The experimental portion of this investigation was conducted in the Ames 7- by 10-Foot Wind Tunnel at a Mach number 0.3 and a Reynolds

number of 2.0 million per foot. This wind tunnel is a subsonic, closed-return, atmospheric tunnel.

The test apparatus included a rectangular wing and vortex generator, mounted on a reflection plane, and a multiple-cone stream survey rake (see figs. 1 and 2). The wing could be pitched about its mid-chord point, although its location on the reflection plane was fixed. Provisions were made for mounting the vortex generators either in the streamwise plane of the wing or 1.5, 3.0, and 4.5 inches above the wing. These vortex generators could be set at several fixed deflection angles (most of the results are for $\alpha_g = 5^\circ$). The leading edge of the wing was 15 inches (5 generator-chord lengths) downstream of the trailing edge of the vortex generator.

The wing was of Fiberglass construction with static-pressure orifices in chordwise rows on the upper and lower surfaces at 12 spanwise stations. A detailed drawing of the wing showing the pressure orifice locations is presented in figure 3.

Three interchangeable vortex generators of rectangular plan form with 3-inch chord and varying span were used (see fig. 1). Each vortex generator was instrumented to measure lift by taking bending moments at two stations near the root. A flat section was used with symmetrical wedges (20° total included angle) for the leading and trailing edges. Because of strength considerations, the vortex generators were tapered in thickness from 3 percent of the chord at the tip to 7, 10, and 12 percent at the root for the 6, 12, and 15-inch-span generators, respectively.

The stream survey rake consisted of five 40° cones instrumented to measure static pressures at four radial points, 90° apart, on the cone and also total pressure at the apex. Details of the rake are shown in figure 4. The rake was sting mounted on a support system which allowed the rake to be translated in the vertical direction (perpendicular to the reflection plane) with the plane of the rake perpendicular to the plane of the wing (see fig. 2). Surveys were made at various streamwise locations by adjusting the length of the string.

TESTS AND PROCEDURES

The entire test was conducted at a constant dynamic pressure of 125 pounds per square foot. All pressures were measured with manometers using water as the fluid. The manometers were photographed and the tube heights read to within ± 0.05 inch with the aid of optical film readers.

The reflection plane was mounted far enough from the tunnel ceiling to exclude effects of the tunnel boundary layer. Stream surveys made in the vicinity of the reflection plane showed a maximum variation

of 1 percent of the dynamic pressure and a stream angle of 0.2° in the downwash direction and no stream angle in the sidewash direction. Corrections for tunnel-wall interference effects on the downwash angles were found to be negligible and so were not included in the results.

A vortical wake was created by the vortex generators. Generators of rectangular plan form were used so the wake would tend to roll up rapidly into a single vortex. Lift produced by the vortex generators was calculated from the bending moment measured by electrical strain gages mounted on the surface of the vortex generators. Tests were made with tufts of yarn attached to the upper surface of the vortex generators to determine the maximum incidence angle allowable without appreciable flow separation.

Static pressures were measured on the upper and lower surfaces of the wings in the uniform stream and in the wake of the vortex generators. Increments of lifting pressure between the data obtained in a vortical wake and in a uniform stream were then integrated over the wing chord to get the induced section-lift coefficients. A spanwise integration of these section-lift coefficients then gave the lift coefficient C_{Li} , induced by the vortical wake. From these results the interference factor, a ratio of induced lift on the wing to the lift produced by the vortex generator, was obtained.

A multiple-probe survey rake was used to measure stream angle in the downwash and sidewash direction and to measure local dynamic pressures. A complete description of the method of calibrating a 40° cone to measure flow angles and total pressure is presented in reference 12. The same calibration technique was used in the present investigation, except that dynamic pressure was obtained from a difference of local static pressure and local total pressure.

Stream surveys were made to locate the vortex and to measure the strength of the circulation in the air stream. The survey rake was moved parallel to the span of the wing and the spanwise increments were varied between data points to adequately define the stream in the vicinity of the vortex core. Spanwise location of the vortex center was shown by a reversal in sign of the downwash angle while the width of the core was taken as the distance between the maximum and minimum downwash angles measured in a plane parallel to the wing at the predicted height of the vortex core. Circulation was obtained by integrating the induced velocity in the transverse plane along rectangular paths which enclosed the complete wake. Repeatability of the data was shown to be 0.5 percent of the dynamic pressure and 0.25° of the downwash or sidewash angles.

RESULTS AND DISCUSSION

Determination of the characteristics of wings or tail surfaces in a nonuniform flow field downstream of a lifting surface consists basically of two parts: first, determination of the stream conditions in the flow field, and second, evaluation of the effect of this nonuniform stream on the trailing surface. In the discussion to follow, both of these features of the problem will be treated by comparing theoretical and experimental results.

The Vortical Wake

A comparison of theoretical and experimental downwash angles in the crossflow plane of the wing leading edge is presented in figure 5 for vortex generators with three different spans. These surveys were made along a line parallel to the vortex generator trailing edge and close to the center of the vortex. Although the strength of the theoretical horseshoe vortex has been chosen to preserve the lift impulse, there is considerable disagreement between the theoretical and experimental downwash angles. It appears that the magnitude and spanwise variation of the theoretical downwash angles (fig. 5) are reasonable but the spanwise location of the theoretical vortex core is displaced from the experimental location. Spanwise vortex locations obtained from the stream-survey data (see fig. 6) are singularly different from the locations predicted by theory. The vortex formed by each of the three vortex generators appears to originate at the tip and then trail back along a nearly streamwise path. It would seem that the location of the vortex is strongly influenced by the small high lift region previously measured at the tip of rectangular wings (see ref. 10, p. 27⁴). Variation of the span load distribution with aspect ratio may have affected the rate at which the vortical wake rolled up, but it did not measurably alter the vortex location.

It should be noted that this discussion on vortex location concerns lifting surfaces of rectangular plan form. If the plan form of the vortex generators had been highly tapered or elliptical, the agreement between theoretical and experimental vortex locations might have been better. Some published experimental data tend to substantiate this plan-form effect. Wind-tunnel data (see ref. 13) obtained at a Mach number of 1.6 with a rectangular wing and experimental apparatus similar to that used in the present investigation locate the trailing vortex nearly in line with the wing tip. In contrast, water-tank tests with elliptical and triangular wings (see ref. 1) show the experimental vortex core approaching the theoretical location several chord lengths downstream of the wing.

In an attempt to find out more about the origin of the vortex, a stream survey was made in the region of the wing tip. The wing was used

A
2
3
2

in this survey because of its larger size and more conventional section than the vortex generator. Surveys were made in the transverse plane at 20, 50, 80, 100, and 115 percent of the wing chord with the wing at an angle of attack of 6° . In figure 7 the experimental vertical location of the vortex center is shown with a half section of the wing drawn in for reference. The vortex location was taken as the apparent center of rotation of the downwash and sidewash velocity vectors in the transverse plane. A well-defined vortex was found which appeared to be shed from the side edge of the wing tip. The importance of this side-edge effect in determining the nature of the wake of a rectangular wing is shown by the strength of this tip vortex which was found by integrating the crossflow velocities around a path which just enclosed the vortex core. At the trailing edge the strength of the tip vortex was nearly half of the entire circulation. In figure 7 the variation of circulation in the chordwise direction is shown to illustrate the manner in which the vortical wake develops. About 70 percent of the total circulation of the wing was encompassed in this survey of the outboard one-fourth of the wing semispan.

The manner in which the wake of a wing rolls up into a trailing vortex in viscous flow is not completely understood. A host of experimental data shows the vortex, at some distance downstream of the lifting surface, to have a core of finite diameter which rotates as a solid body. An approximation for calculating vortex location and core size is presented in reference 1. However, this method predicts vortex-core diameters which are considerably larger than those obtained experimentally by stream surveys.

Vortex-Wing Interference

The interference factors obtained by various theoretical methods are shown in figure 8 as functions of the span of the vortex-generator relative to the span of the wing. The experimental interference factors obtained with a vortex-generator angle of attack of 5° are shown for comparison. The classical strip theory is obviously in error near the ratio of $b_G/b_W = 1$. Strip theory fails to take account of the loss of lift effectiveness of those elements of the wing near the tip. The infinite velocities near the center of the vortex and the finite lift at the wing tip prescribed by strip theory result in excessively large interference factors when the vortex passes near the wing tip. The results of figure 8 show that if the span of the forward surface is less than about two-thirds of the span of the following wing, strip theory can be used to predict the interference load with reasonable accuracy. The infinite interference factor is avoided in the reverse-flow theory since the loading function goes to zero at the wing tip. Also, modification of the reverse-flow computations to include a finite vortex-core diameter effects a sizable improvement when the vortex core passes near the wing tip and the calculated interference factors come into good agreement with experiment.

The effect of the discrepancy between the theoretical and experimental vortex location (fig. 6), in terms of the magnitude of the interference factor, is illustrated in figure 9. The interference factors were computed for $\alpha_G = 5^\circ$ using the reverse-flow theory, assuming a finite vortex-core diameter, for three spanwise locations of the vortex: (1) streamwise from the generator tip, (2) the location indicated theoretically, and (3) the location measured experimentally.

It is apparent in figure 9 that correlation between theory and experiment is very good for the vortex either trailing from the tip or at its experimental location. Use of lifting-line theory to predict the vortex location results in sizable errors when the span of the forward surface is such that its vortex passes near or outboard of the tip of the following surface.

Effect of vortex height above wing.— Variation of the interference factor with the height of the vortex generator above the wing-chord plane calculated by the reverse-flow theory, including a finite core, agrees quite well with experimental values as shown in figure 10. However, the experimental interference factors obtained for various vertical distances (z_G), showed one interesting effect which was not accounted for by the theory. The experimental interference factors obtained with a positive value of α_G reach a maximum value at $z_G/c_W \approx 0.25$ while the theoretical maximum, assuming the trailing vortex to be symmetrical in the vertical plane, occurs at the wing-chord plane. It is well known that the wake of a lifting surface starts out as a vortex sheet which proceeds to roll up into a spiral while progressing downstream. The spiral develops quite rapidly, but only asymptotically approaches the fully rolled-up vortex assumed in the line-vortex theory. In these tests, the vortex generator at a positive incidence produced a counterclockwise spiral (looking downstream) with the tail of the spiral moving downward. It would seem, from the results presented in figure 10, that the small part of the vortex sheet which is not yet rolled up contributes a measurable part of the interference load.

A sample calculation was made to substantiate this reasoning. Three horseshoe vortices were used to simulate the distributed vortical wake. The vortices were distributed according to the theoretical spanwise loading, and the numerical stepwise integration procedure of reference 2 was used to locate the vortices in the transverse plane at the wing leading edge. Interference factors obtained by this theoretical method are presented in figure 10(a) for the vortex generator located plus and minus 1.5 inches from the wing-chord plane. These results are in better agreement with experiment than those of the single-vortex theory. Thus, it can be surmised that the wake could be more accurately described by a greater number of vortices properly distributed. This method is not recommended except in unusually detailed studies since the number of computations necessary to determine the vortex location varies as the square of the number of horseshoe vortices considered.

Effect of wing angle of attack.- Calculations of vortex interference on a wing by two-dimensional line-vortex theory at other than zero angle of attack require some additional assumptions. First, a streamwise vortex is not parallel to the surface of a wing at angle of attack. Further, since the vortex is deflected to some extent by the wing flow field, the variation of the distance to the vortex along the wing chord is unknown. In this investigation the height of the vortex was arbitrarily taken as the perpendicular distance between the mid-chord point of the wing and the undisturbed path of the vortex. Fortunately, the vortex height is not critical since the incidence of the wing is usually a small angle and the computation of induced loads is fairly insensitive to small changes in z_G .

The experimental interference factors obtained with a vortex generator of half the wing span are presented in figure 11 for an α_W range of -4° to $+6^\circ$. The experimental results show that with the wing at angle of attack, the induced loads are dependent upon the direction of circulation. The interference factors are larger when α_W and α_G are of the same sign than when they are of opposite sign. For a wing angle of attack of 4° , this difference amounts to about one-fourth of the interference factor at zero angle of attack. The Prandtl lifting-line theory agrees with the experimental trend shown in figure 11 while the reverse-flow theory fails to show this trend.

Distribution of vortex-induced loads.- Theoretical prediction of the distribution of vortex-induced loads is somewhat more difficult than the calculation of the total vortex interference. The spanwise induced load distributions obtained by the lifting-line theory and the Weissinger method are compared to the experimental induced loads in figure 12. Measured downwash angles were used in the computations to eliminate the uncertainties in the theoretical vortex. The method of reference 10 for calculating spanwise lift distribution determines the circulation distribution which satisfies the downwash angles prescribed for a number of control points on the wing. Thus the mutual influence of the control points as well as the plan form of the wing is considered in these computations. Considering the fact that linearized two-dimensional theory was used, the agreement with experiment (fig. 12) is fairly good. The Weissinger method predicts the vortex-induced loads better than the lifting-line theory, especially for the wing in the wake of the 6-inch vortex generator where the downwash field was most nonuniform.

Surprisingly good agreement between the theory, using Weissinger's method, and experiment is shown in figure 13 for those cases where the vortex generators were not in the chord plane of the wing. In those cases where experimental downwash angles were available, the results in figure 13 show that a line vortex, with a finite core, trailing from the tip is a reasonable representation of the actual downwash field.

Although existing methods predict the spanwise distribution of loads within the limitations of two-dimensional theory, no suitable

theoretical method was found for predicting the chordwise variation of induced loads at subsonic speeds. However, the pressure distributions presented in figure 14 illustrate the experimental chordwise variations obtained in this investigation. Dashed portions of the curves represent extrapolations of the data in regions where the lifting pressures varied rapidly between chordwise rows of pressure orifices. The chordwise distribution of lifting pressures over the region inboard of the vortex core looks very much like that obtained in two-dimensional flow. However, in the region where the vortex core passes over the wing, the induced loads are concentrated near the wing leading edge. Although the local chordwise center of pressure varied widely in the region of the vortex, the center of pressure of the total induced load was never more than 3 percent of the chord away from the quarter-chord point of the wing for any of the test conditions.

At the leading edge (see fig. 14), the vortex location is evident by the reversal of the induced loads. However, downstream of the leading edge the pressure contours cannot be used to trace the vortex path because of the mutual effects of the induced pressures acting over the entire wing. Stream-survey data obtained one chord length behind the wing showed that the spanwise location of the vortex did not change appreciably in passing the wing, even with the wing at an angle of attack of 6° .

CONCLUDING REMARKS

The aerodynamic loads induced on a rectangular wing by a vortical wake have been obtained for a number of vortex positions, both spanwise and normal to the wing, and for the wing at several angles of attack. Comparisons were made between the experimental results, and predictions were made with available theoretical methods. In addition, a stream survey was made of flow angles in the vortical wake.

Stream-survey results showed that the wake of lifting surfaces of rectangular plan form starts to roll up quickly forming a vortex which trails back in a nearly streamwise direction from the wing tip rather than from the centroid of circulation predicted by the lifting-line theory. This result is believed to be restricted to essentially untapered plan forms.

Results of the investigation indicated that the vortex interference lift could be predicted over the range of test variables by the reverse-flow theory if a vortical wake with a finite-core diameter were considered. The accuracy of the theoretical predictions was relatively insensitive to the choice of spanwise vortex position, except when the vortex core passed immediately outboard of the wing tip.

The experimental induced loads on the wing at zero angle of attack when the vortex was not in the wing-chord plane were different for a positive and negative direction of circulation because of the asymmetry of the vortex sheet which was not fully rolled up. When the wing was at angle of attack the direction of circulation, regardless of extent of roll-up, also affected the magnitude of the induced loads. In this case, the induced load was greater when the vorticity was in the same sense as that shed by the wing itself.

The spanwise distribution of vortex-induced loads was predicted by lifting-line theory with reasonable accuracy using either the measured downwash angles or the values calculated for a potential vortex trailing back from the tip of the vortex generators. Use of Weissinger's modification to the theory improved the accuracy of the predictions.

Ames Research Center
National Aeronautics and Space Administration
Moffett Field, Calif., July 19, 1960

REFERENCES

1. Spreiter, John R., and Sacks, Alvin H.: The Rolling-Up of the Trailing Vortex Sheet and Its Effect on Downwash Behind Wings. Jour. Aero. Sci., vol. 18, no. 1, Jan. 1951, pp. 21-32, 72.
2. Rogers, Arthur W.: Application of Two-Dimensional Vortex Theory to the Prediction of Flow Fields Behind Wings of Wing-Body Combinations at Subsonic and Supersonic Speeds. NACA TN 3227, 1954.
3. Spahr, J. Richard, and Dickey, Robert R.: Wind-Tunnel Investigation of the Vortex Wake and Downwash Field Behind Triangular Wings and Wing-Body Combinations at Supersonic Speeds. NACA RM A53D10, 1953.
4. Pitts, William C., Nielsen, Jack N., and Kaattari, George E.: Lift and Center of Pressure of Wing-Body-Tail Combinations at Subsonic, Transonic, and Supersonic Speeds. NACA Rep. 1307, 1957.
5. Grigsby, Carl E.: The Use of the Rolled-Up Vortex Concept for Predicting Wing-Tail Interference and Comparison With Experiment at Mach Number of 1.62 for a Series of Missile Configurations Having Tandem Cruciform Lifting Surfaces. NACA RM L52H05, 1952.
6. Edwards, S. Sherman: Experimental and Theoretical Study of Factors Influencing the Longitudinal Stability of an Air-To-Air Missile at a Mach Number of 1.4. NACA RM A51J19, 1952.

7. Heaslet, Max. A., and Spreiter, John R.: Reciprocity Relations in Aerodynamics. NACA Rep. 1119, 1953.
8. Lawrence, H. R.: The Lift Distribution on Low Aspect Ratio Wings at Subsonic Speeds. Jour. Aero. Sci., vol. 18, no. 10, Oct. 1951, pp. 683-695.
9. Jones, Robert T., and Cohen, Doris: Aerodynamics of Wings at High Speeds. Vol. VII of High Speed Aerodynamics and Jet Propulsion, Div. A, ch. 2, p. 77. A. F. Donovan and H. R. Lawrence, editors.
10. von Mises, Richard: Theory of Flight. 1st ed., McGraw-Hill Book Co., Inc., New York, 1945.
11. Weissinger, J.: The Lift Distribution of Swept-Back Wings. NACA TM 1120, 1947.
12. Centolanzi, Frank J.: Characteristics of a 40° Cone for Measuring Mach Number, Total Pressure, and Flow Angles at Supersonic Speeds. NACA TN 3967, 1957.
13. Davis, Theodore: The Measurement of Downwash and Sidewash Behind a Rectangular Wing at a Mach Number of 1.6. Jour. Aero. Sci., vol. 19, no. 5, May 1952, pp. 329-332, 340.

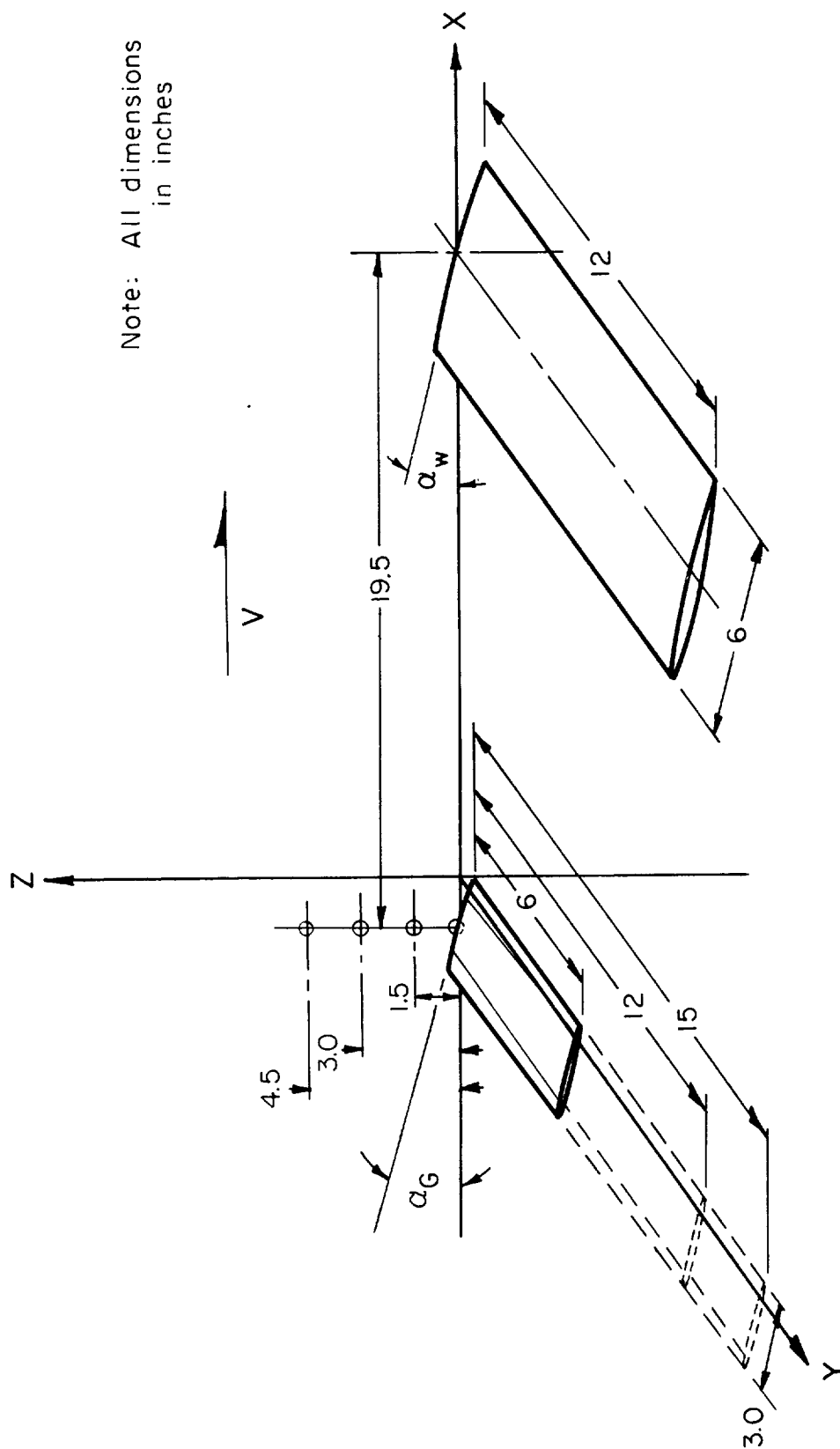
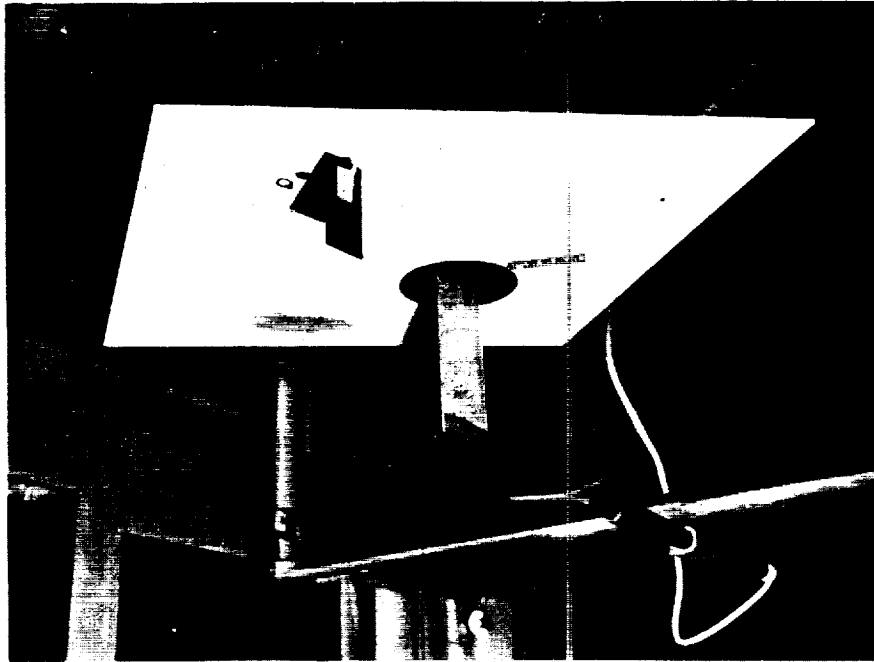


Figure 1.- Schematic diagram of apparatus showing system of axes.



A-23696

Figure 2.- Test apparatus installed in the Aies 7- by 10-Foot Wind Tunnel.

A
C
C
E
S
S

Wing orifice locations			
Sta. no.	$\frac{y}{s}$	Sta. no.	$\frac{y}{s}$
1.	.02	7.	.60
2.	.12	8.	.70
3.	.20	9.	.80
4.	.30	10.	.85
5.	.40	11.	.90
6.	.50	12.	.95

NACA 0006-63 Wing section
pressure orifices on upper and
lower surfaces at: -.03, .05, .10,
.15, .20, .25, .30, .40, .50, .60, .75
and $.88 \frac{x}{c}$

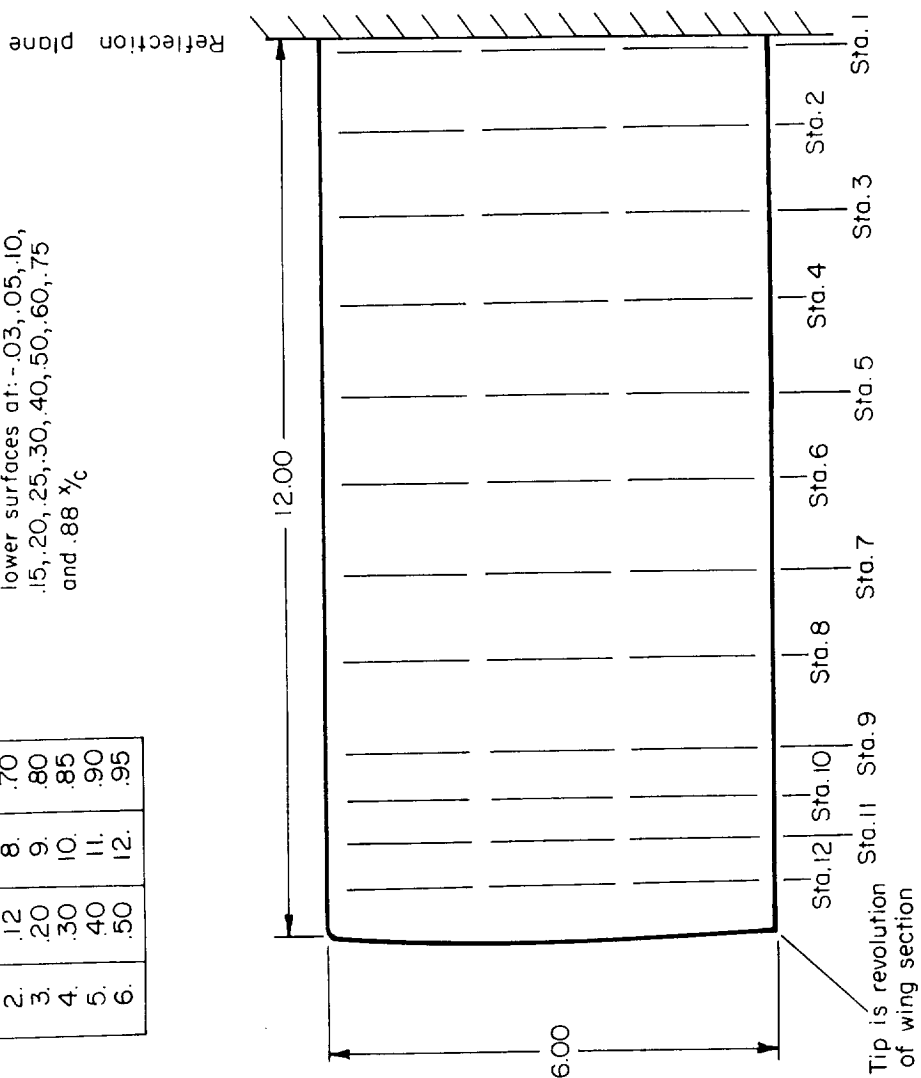


Figure 3.- Wing details and pressure orifice locations.

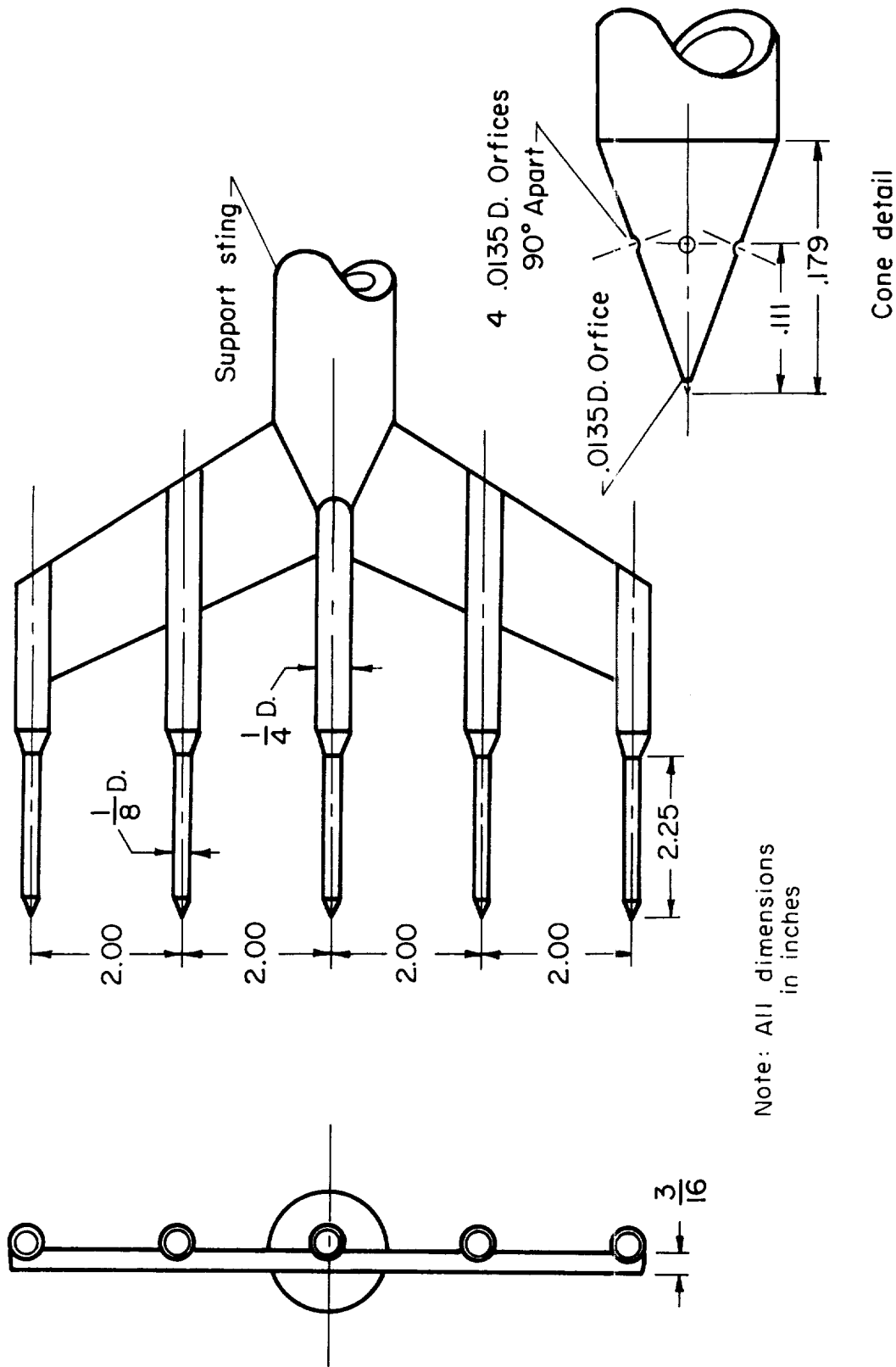


Figure 4.- Dimensional sketch of survey rake.

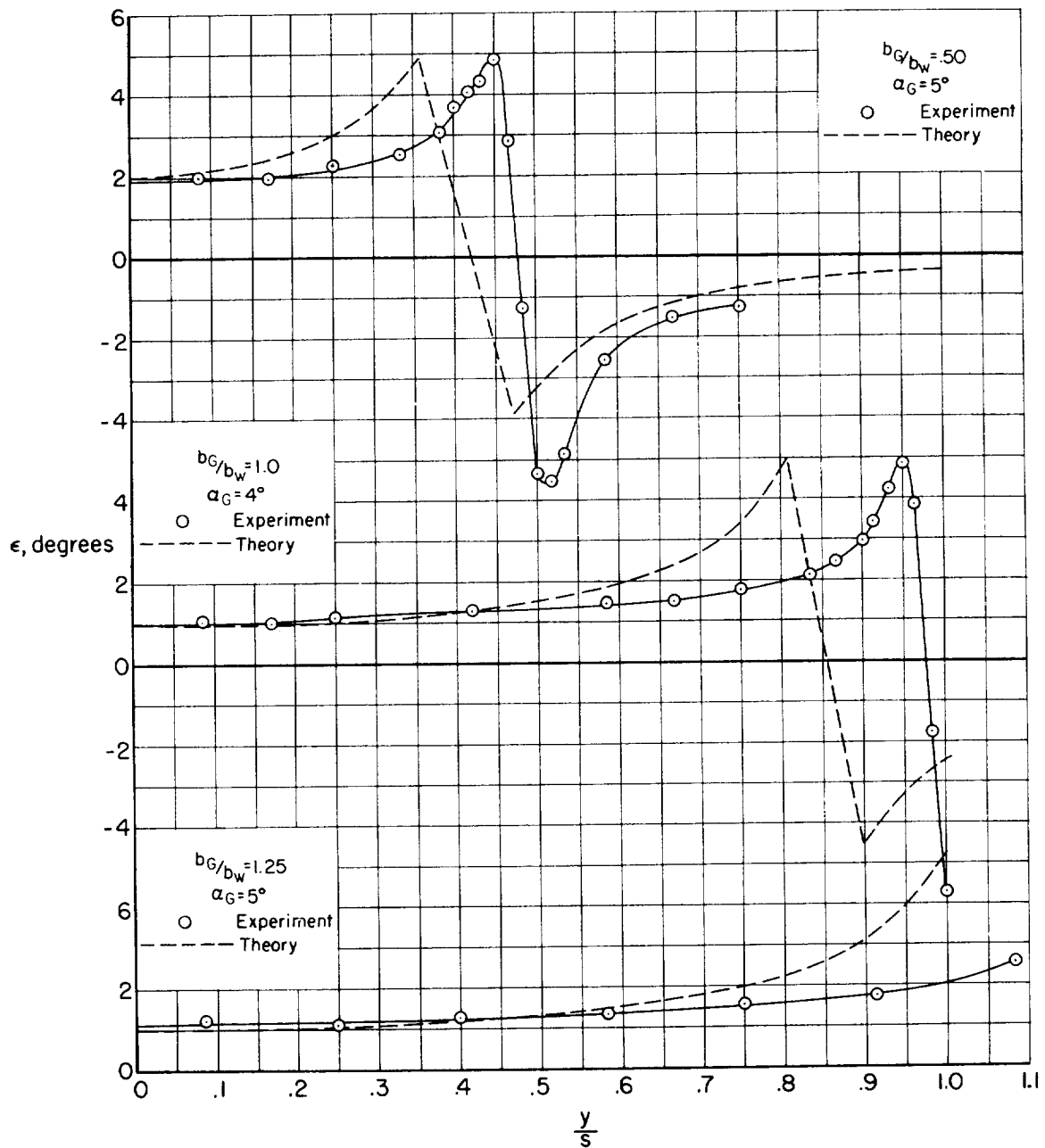


Figure 5.- Spanwise distribution of downwash angle behind three rectangular vortex generators; $x = 15$ in., $z_G = 0.28$ in.

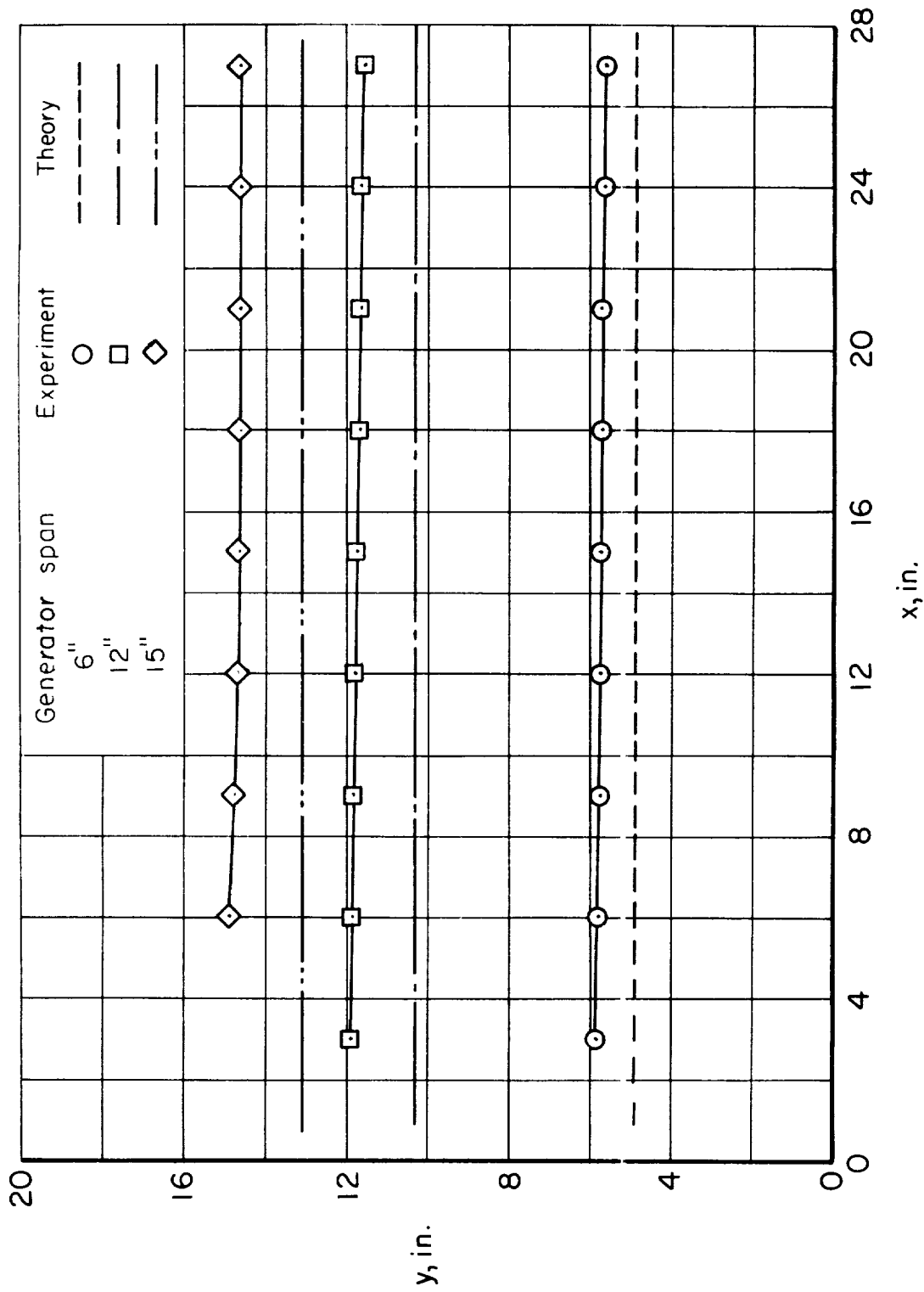


Figure 6.-- Comparison of theoretical and experimental spanwise vortex locations; $\alpha_g = 5^\circ$.

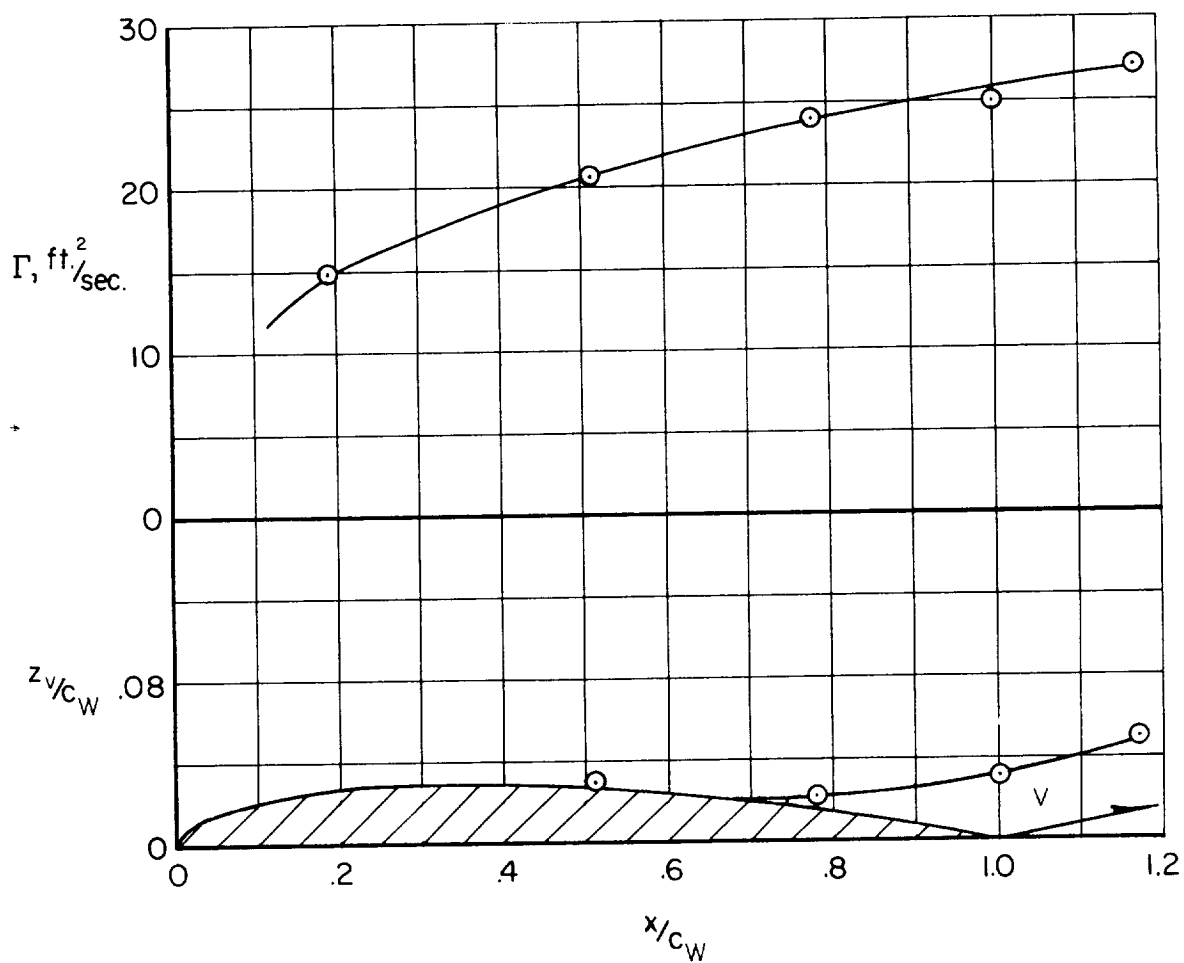


Figure 7.- Development of circulation near the wing tip and vortex path;
 $\alpha_W = 6^\circ$.

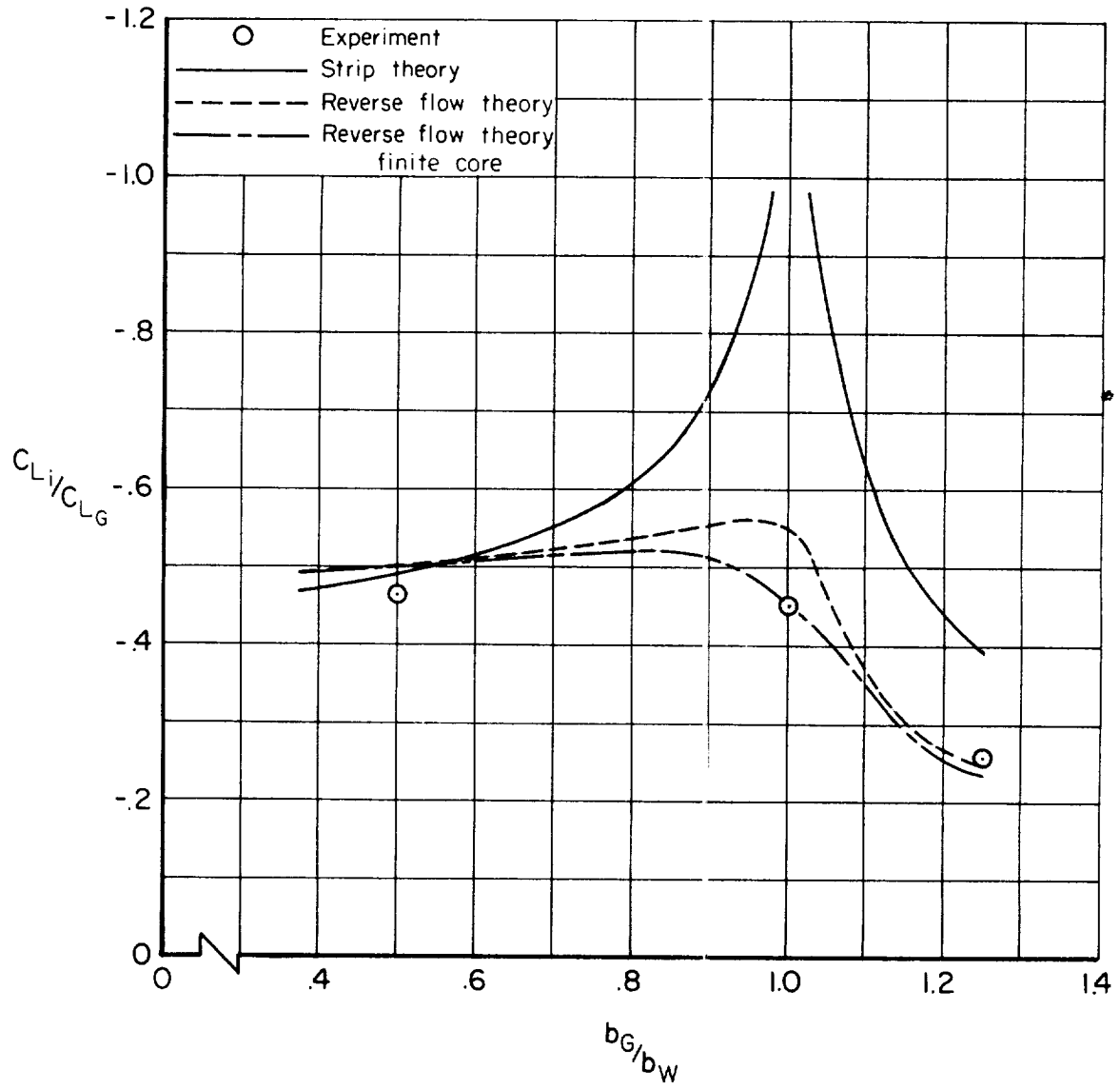


Figure 8.- Comparison of experimental and theoretical interference factors using tip location for vortex; $\alpha_W = 0^\circ$, $z_G = 0$.

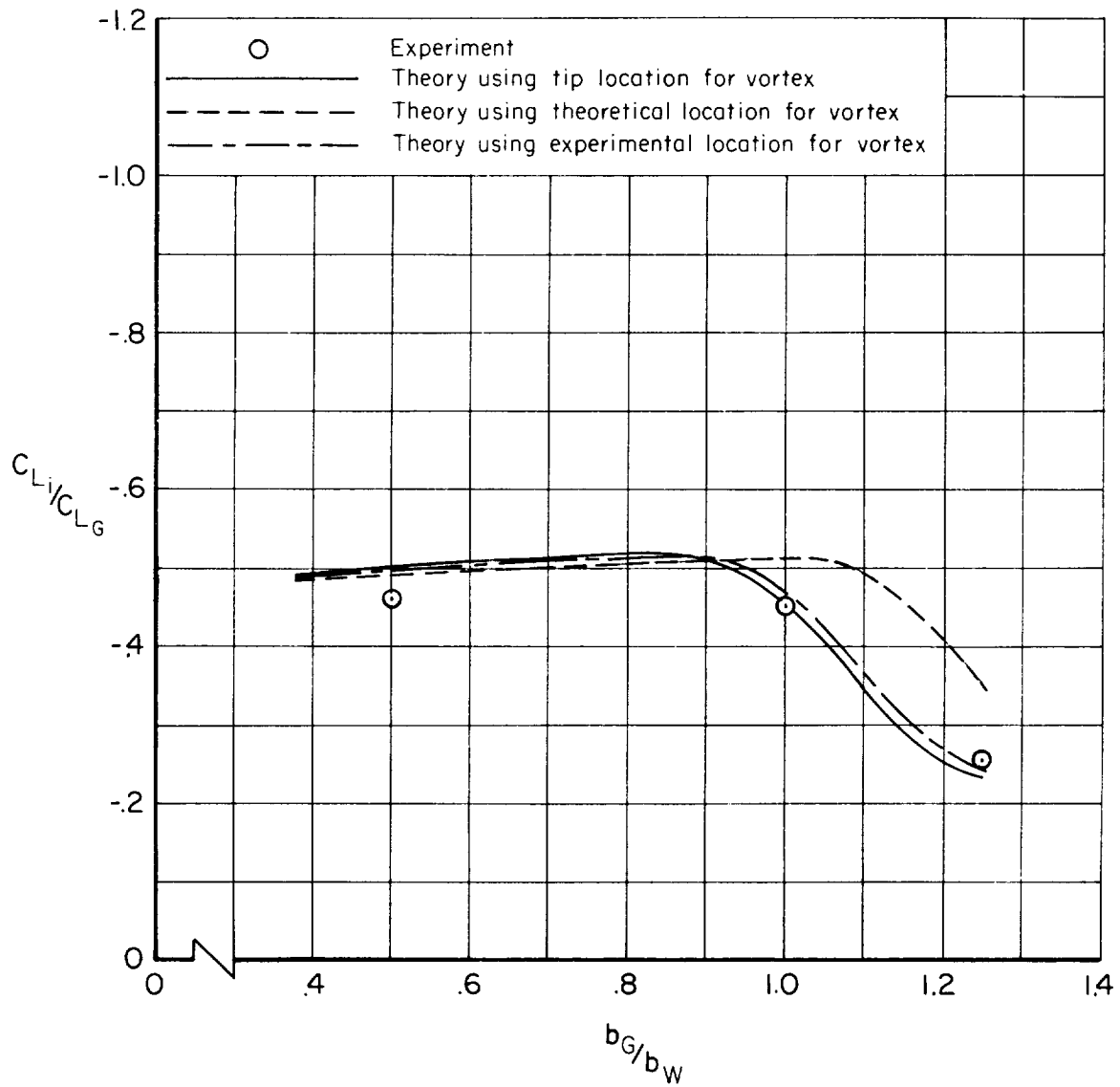
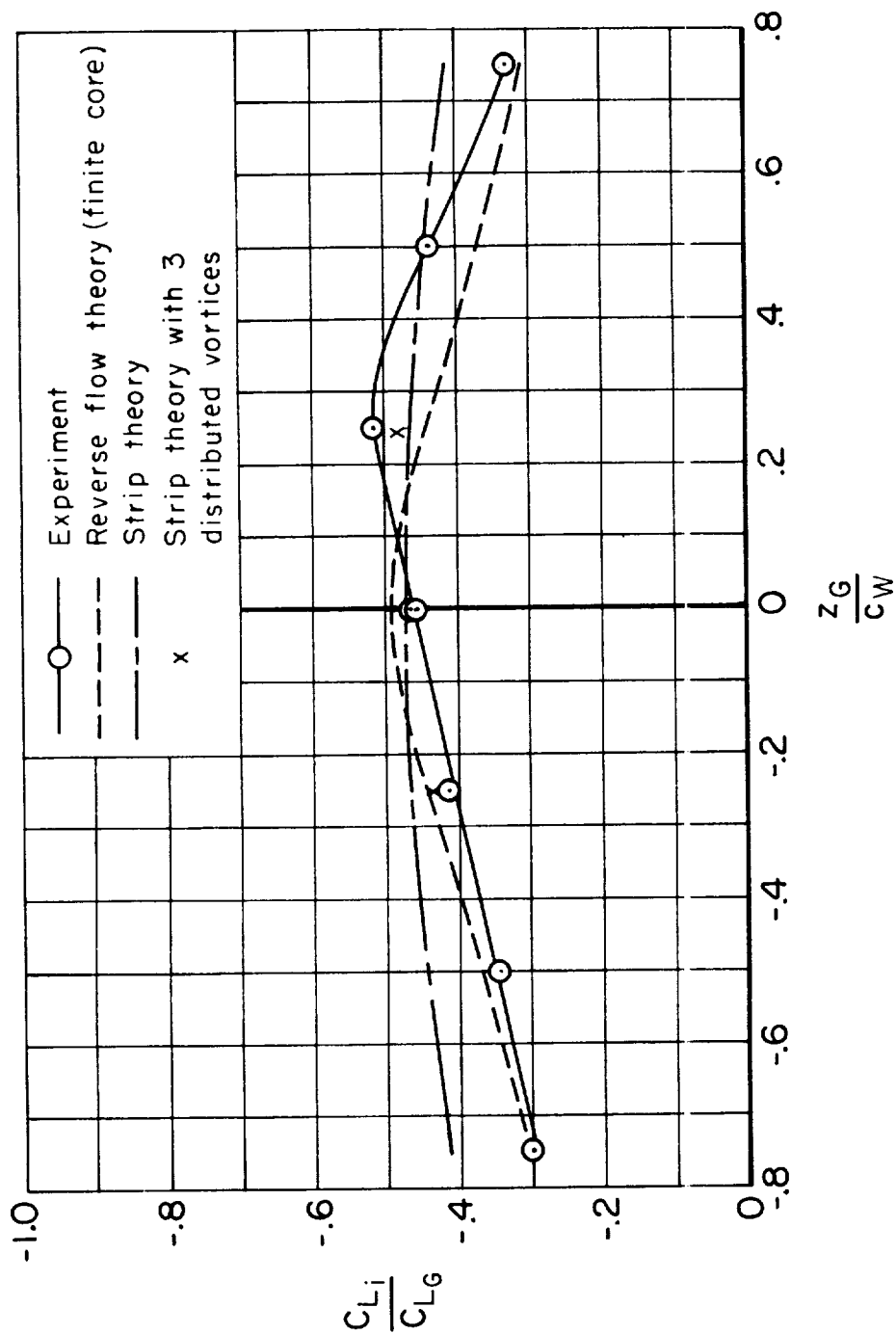
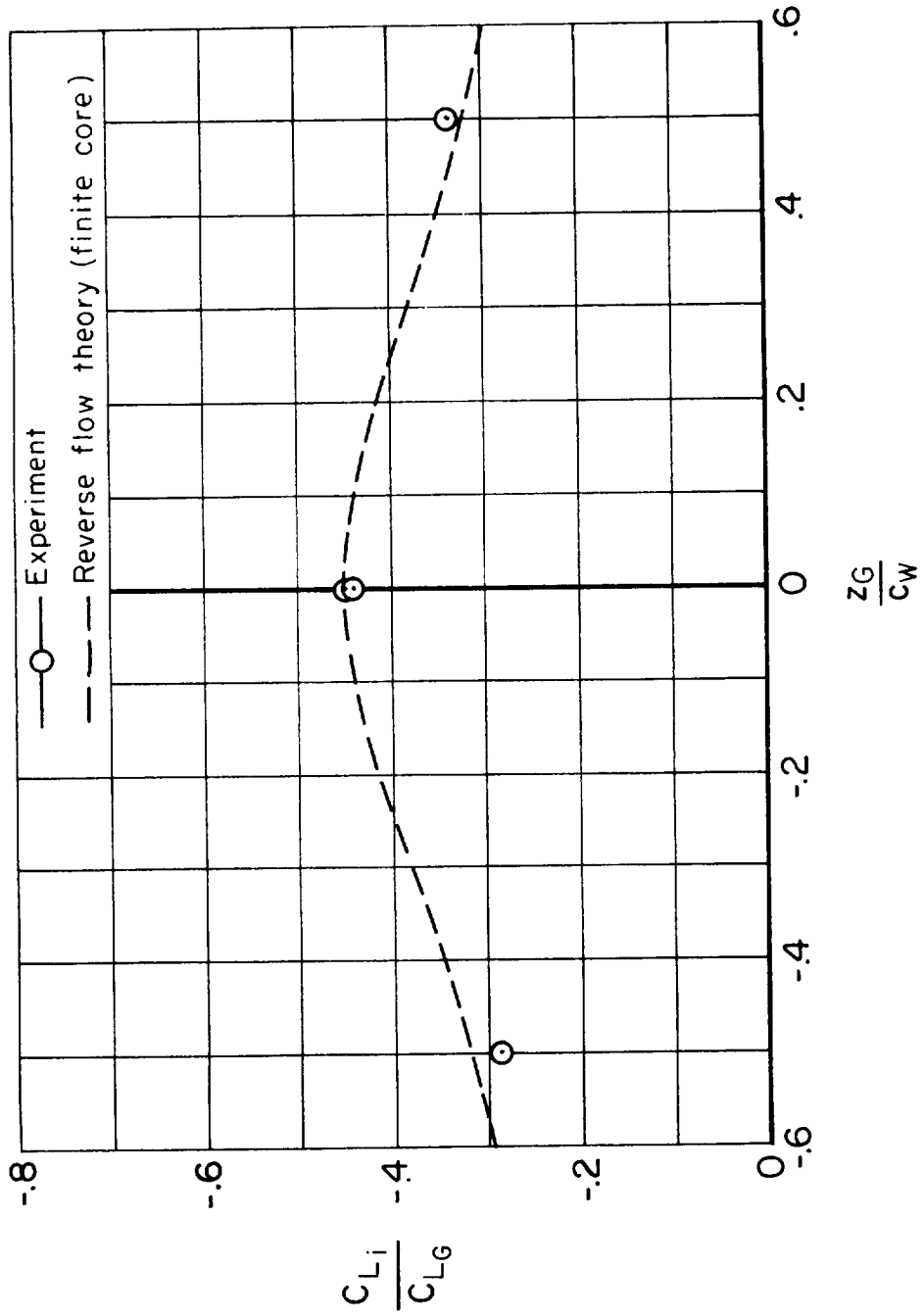


Figure 9.- Comparison of experimental and theoretical interference factors for several vortex locations using reverse flow theory (finite core); $\alpha_W = 0^\circ$, $z_G = 0$.



(a) $b_g/b_w = 0.5$

Figure 10.- Effect of vortex generator height on interference factor;
 $\alpha_w = 0^\circ$.



(b) $b_G/b_W = 1.0$

Figure 10.- Concluded.

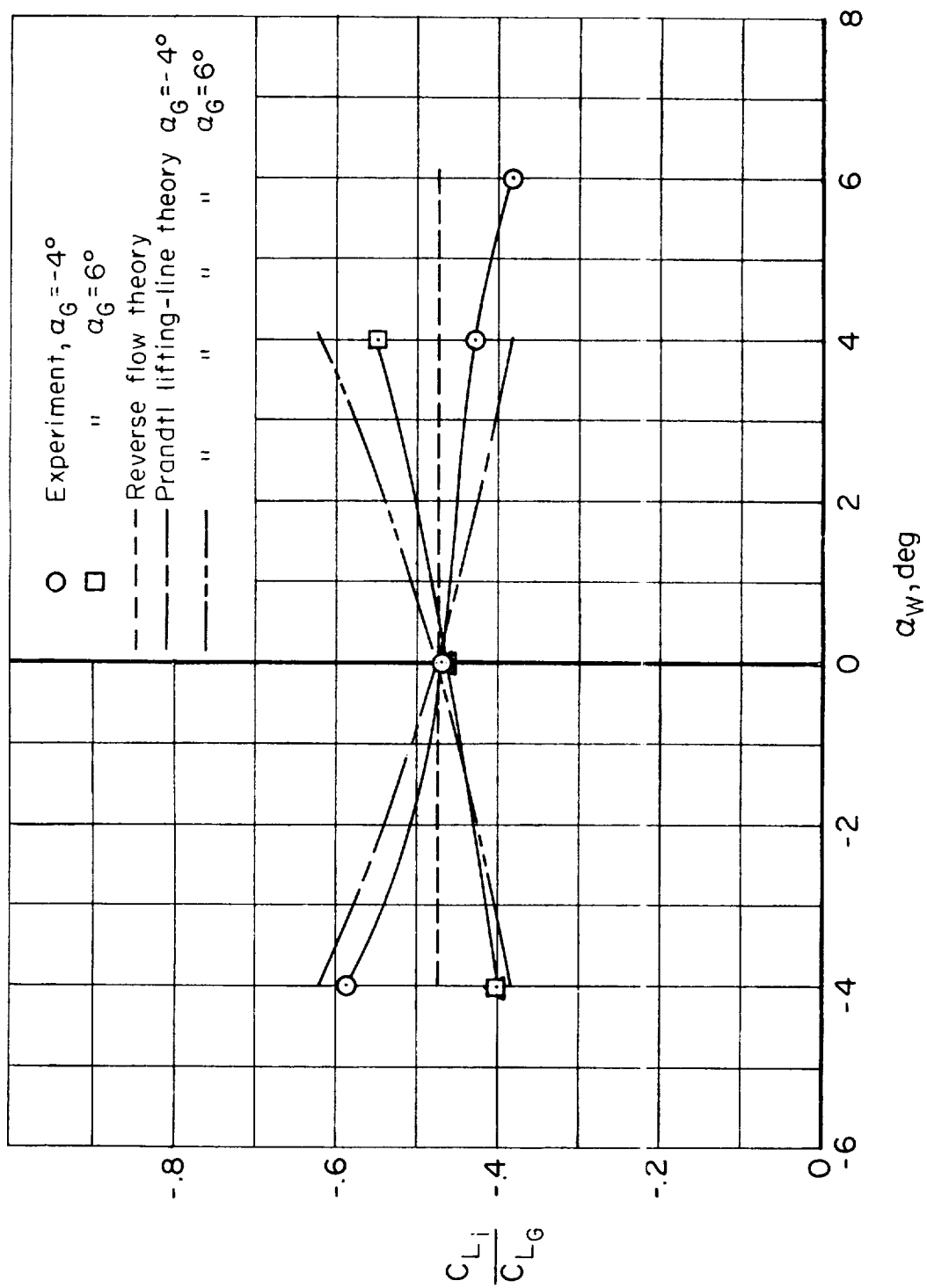


Figure 11.- Effect of wing angle of attack on interference factor;
 $b_G/b_W = 0.5$, $z_G = 0$.

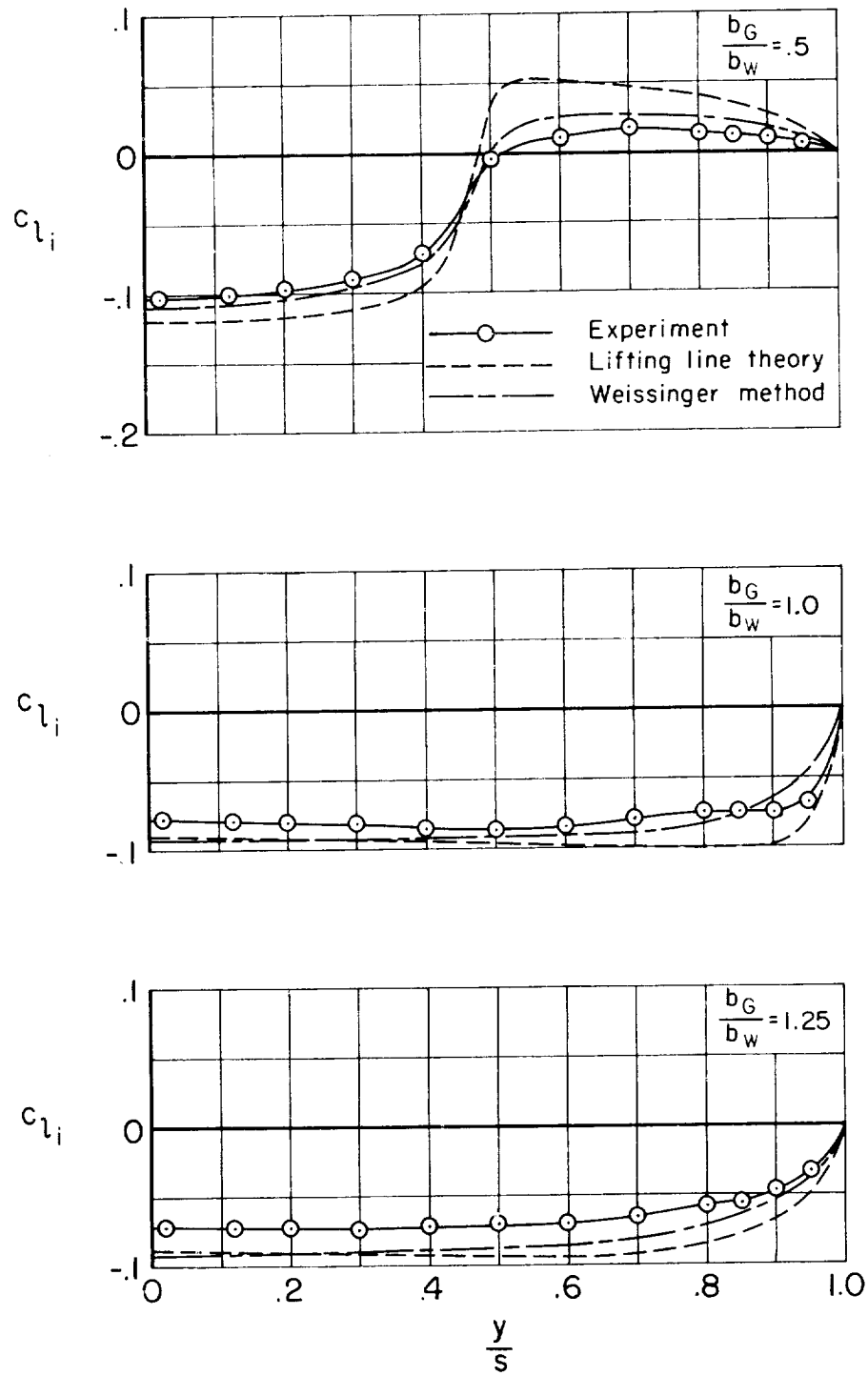


Figure 12.- Comparison of experimental and theoretical spanwise distribution of vortex-induced loads using experimental downwash angles; $\alpha_W = 0^\circ$, $\alpha_G = 5^\circ$, $\alpha_G = 0$.

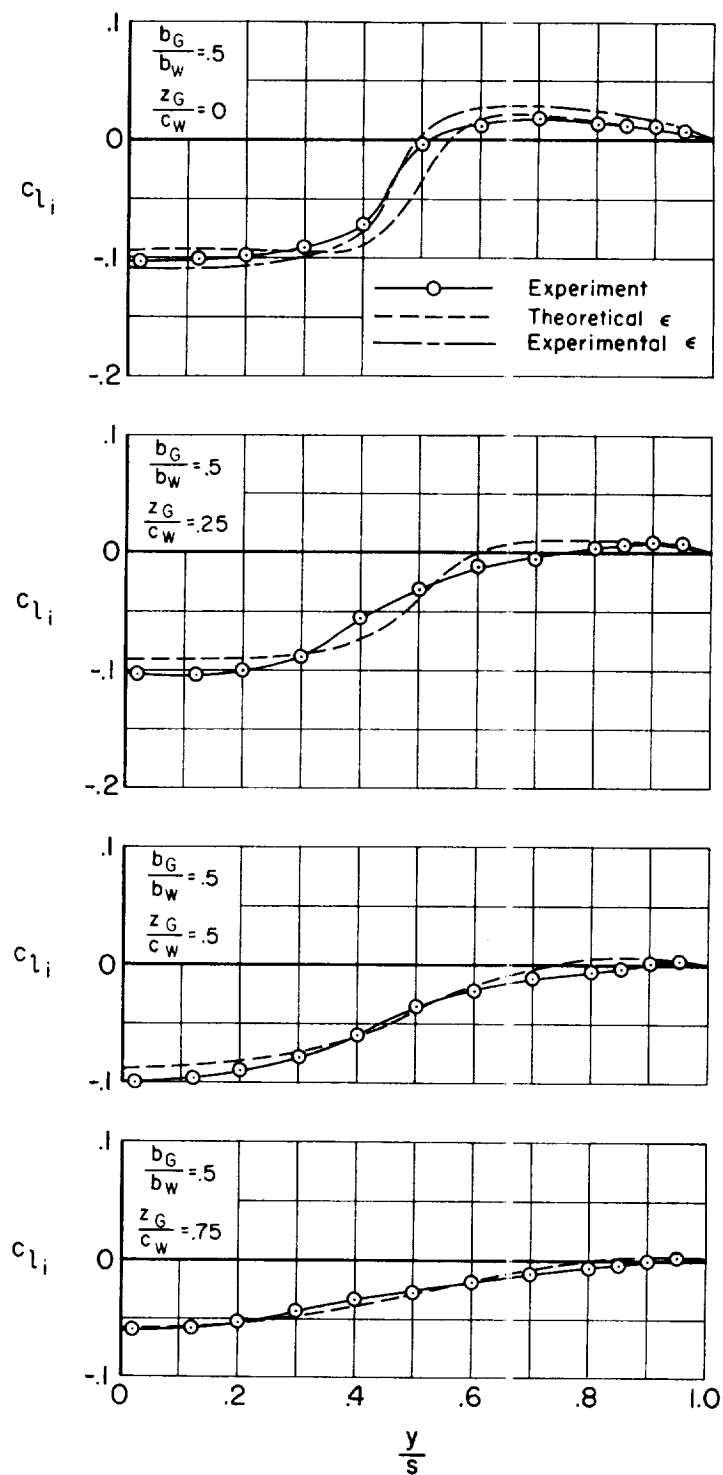
A
2
8
2

Figure 13.- Spanwise distribution of vortex-induced loads by the Weissinger method with experimental and theoretical downwash angles; $\alpha_W = 0^\circ$, $\alpha_G = 5^\circ$.

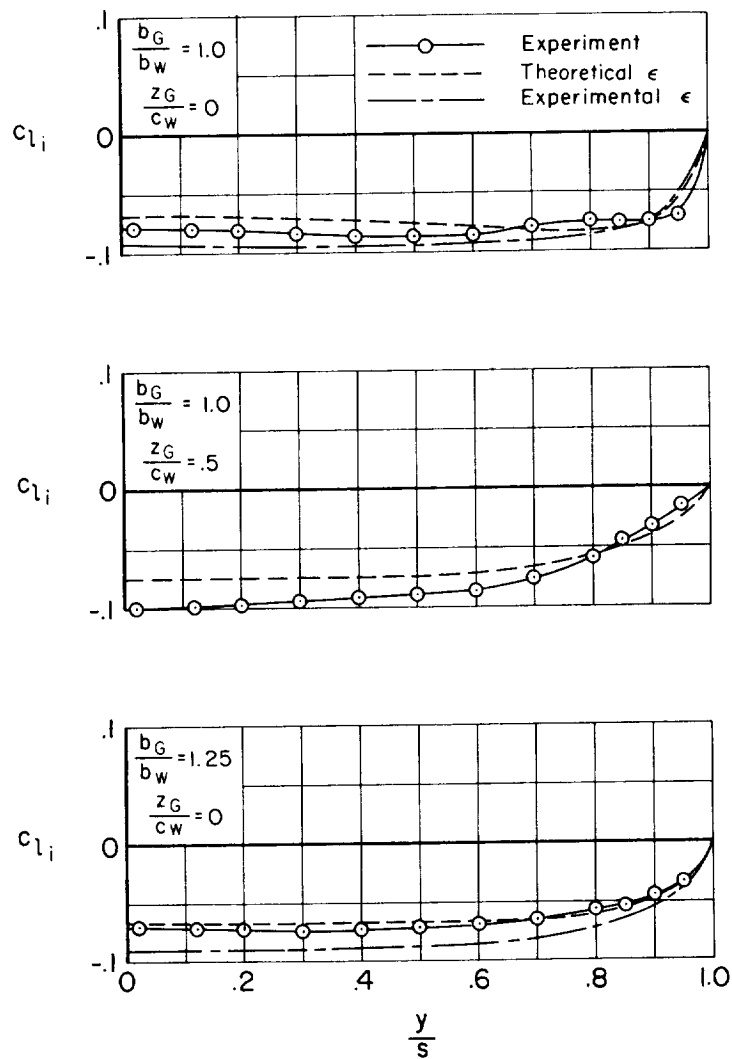


Figure 13.- Concluded.

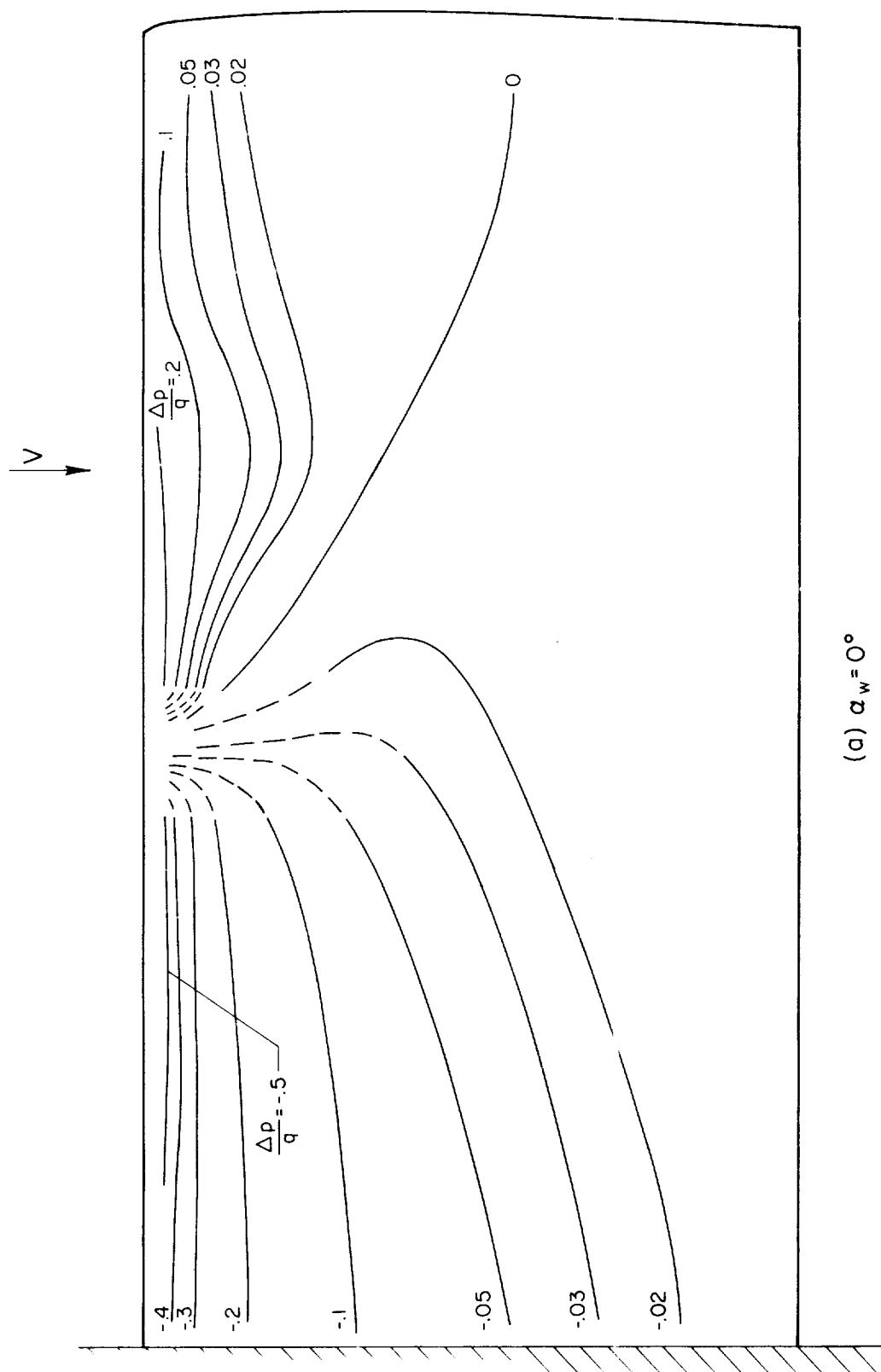
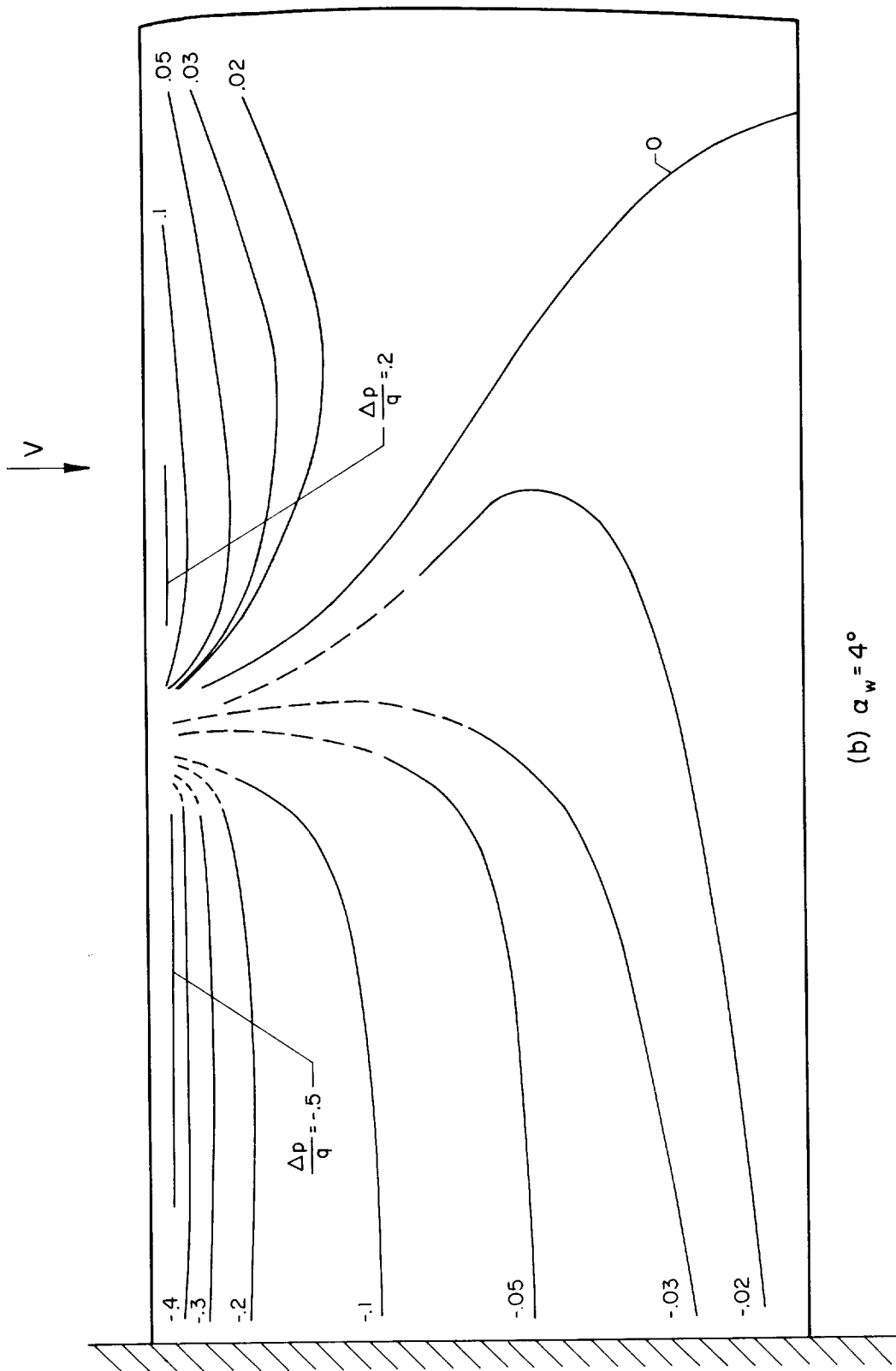


Figure 14.- Induced lifting pressure contours over plan form of wing in the wake of a vortex generator; $\alpha_G = 5^\circ$, $z_G = 0$, $b_G/b_W = 0.5$.



(b) $\alpha_w = 4^\circ$

Figure 14.- Concluded.

<p>NASA TN D-339 National Aeronautics and Space Administration. EXPERIMENTAL AND THEORETICAL STUDY OF A RECTANGULAR WING IN A VORTICAL WAKE AT LOW SPEED. Willard G. Smith and Frank A. Lazzeroni. October 1960. 33p. OTS price, \$1.00. (NASA TECHNICAL NOTE D-339)</p> <p>Experimental effects of a vortical wake on a trailing rectangular wing at subsonic speed were determined from measurements of the static pressures on the wing. Location of the vortex relative to the wing was systematically varied as well as the angle of attack of the wing. The vortex generator and wing were mounted on a reflection plane to avoid body-wing interference. A comparison is made between theory and experiment for vortex paths, induced lift, and spanwise induced load distribution.</p>	<p>I. Smith, Willard G. II. Lazzeroni, Frank A. III. NASA TN D-339 (Initial NASA distribution: 3, Aircraft.)</p>	<p>NASA TN D-339 National Aeronautics and Space Administration. EXPERIMENTAL AND THEORETICAL STUDY OF A RECTANGULAR WING IN A VORTICAL WAKE AT LOW SPEED. Willard G. Smith and Frank A. Lazzeroni. October 1960. 33p. OTS price, \$1.00. (NASA TECHNICAL NOTE D-339)</p> <p>Experimental effects of a vortical wake on a trailing rectangular wing at subsonic speed were determined from measurements of the static pressures on the wing. Location of the vortex relative to the wing was systematically varied as well as the angle of attack of the wing. The vortex generator and wing were mounted on a reflection plane to avoid body-wing interference. A comparison is made between theory and experiment for vortex paths, induced lift, and spanwise induced load distribution.</p>	<p>I. Smith, Willard G. II. Lazzeroni, Frank A. III. NASA TN D-339 (Initial NASA distribution: 3, Aircraft.)</p>
<p>NASA TN D-339 National Aeronautics and Space Administration. EXPERIMENTAL AND THEORETICAL STUDY OF A RECTANGULAR WING IN A VORTICAL WAKE AT LOW SPEED. Willard G. Smith and Frank A. Lazzeroni. October 1960. 33p. OTS price, \$1.00. (NASA TECHNICAL NOTE D-339)</p> <p>Experimental effects of a vortical wake on a trailing rectangular wing at subsonic speed were determined from measurements of the static pressures on the wing. Location of the vortex relative to the wing was systematically varied as well as the angle of attack of the wing. The vortex generator and wing were mounted on a reflection plane to avoid body-wing interference. A comparison is made between theory and experiment for vortex paths, induced lift, and spanwise induced load distribution.</p>	<p>I. Smith, Willard G. II. Lazzeroni, Frank A. III. NASA TN D-339 (Initial NASA distribution: 3, Aircraft.)</p>	<p>NASA TN D-339 National Aeronautics and Space Administration. EXPERIMENTAL AND THEORETICAL STUDY OF A RECTANGULAR WING IN A VORTICAL WAKE AT LOW SPEED. Willard G. Smith and Frank A. Lazzeroni. October 1960. 33p. OTS price, \$1.00. (NASA TECHNICAL NOTE D-339)</p> <p>Experimental effects of a vortical wake on a trailing rectangular wing at subsonic speed were determined from measurements of the static pressures on the wing. Location of the vortex relative to the wing was systematically varied as well as the angle of attack of the wing. The vortex generator and wing were mounted on a reflection plane to avoid body-wing interference. A comparison is made between theory and experiment for vortex paths, induced lift, and spanwise induced load distribution.</p>	<p>I. Smith, Willard G. II. Lazzeroni, Frank A. III. NASA TN D-339 (Initial NASA distribution: 3, Aircraft.)</p>

NASA

Copies obtainable from NASA, Washington

NASA

Copies obtainable from NASA, Washington

NASA

Copies obtainable from NASA, Washington

NASA

Copies obtainable from NASA, Washington

